CONSTRUCTIVE THEORY
OF FUNCTIONS'84
Sofia, 1984, p. 382-391

КОНСТРУКТИВНАЯ ТЕОРИЯ
ФУНКЦИЙ'84
София, 1984, с. 382—391

ON THE STRUCTURE OF FINITE ELEMENT SOLENOIDAL SUBSPACES

Karl Gustafson

1. Introduction. The velocity vector field v of a viscous incompressible fluid motion is described by the Navier-Stokes equations

$$v_t - \nu\Delta v + v\cdot\nabla v = -\nabla p \quad \text{in} \quad \Omega \tag{1.1}$$

$$\nabla\cdot v = 0 \quad \text{in} \quad \Omega \tag{1.2}$$

$$v = g \quad \text{on} \quad \partial\Omega \tag{1.3}$$

Here we assume Ω is a piecewise smooth bounded domain in two or three dimensions in which the fluid is moving. We have assumed in (1.1) that there are no body forces. We have also assumed Dirichlet boundary data (1.3) although other boundary conditions can be considered in a similar way. Equation (1.1) is called the momentum equation and equation (1.2) the incompressibility constraint. Equation (1.2) also is called the solenoidal property of v or that v be divergence-free.

The numerical approximation of the Navier-Stokes equations is currently a very important problem. For example, a current goal of aircraft industries is the solution of the Navier-Stokes equations about complete aircraft bodies. For low mach numbers, e.g., less than 0.8, the incompressibility condition may be assumed to hold. There are other important applications, e.g., in chemical reactors and gas dynamics, in which the numerical apprpoximation of the Navier-Stokes equations are important. In many of these equations, (1.2) must be replaced by a more general continuity equation allowing compressibility and changes in density, and equation (1.1) must allow temperature dependence. We will not get into such matters here.

We will, however, make the general claim that the numerical analysis of such equations and problems is in its infancy. This is to be contrasted with the large amount of numerical computation and simulation that is going on. A very large need in this current modelling of flows by such equations is numerical analysis and in particular some good error estimates. From the point of view of approximation

theory, this could be described as the analysis of piecewise polynomial fits to a nonlinear equation in higher dimensions.

2. Finite element approximations. The domain Ω is broken down into triangles (n=2) or tetrahedra (n=3). Let us assume for simplicity that $\partial\Omega$ is already (by an approximation) a piecewise flat boundary, so that all of Ω is encompassed by the triangulation with elements. On each element τ one specifies an approximating function, usually a polynomial of low order. There may or may not be continuity and differentiability conditions across element boundaries.

Following [2] which follows [1], our approach to the numerical discretization of the Navier-Stokes equations is based on:

(a) first require that the approximations on Ω satisfy a discrete version of the solenoidal condition (1.2)

(b) then advance the discretized momentum equation to the next time step.

Here we shall discuss principally step (a) only.

For other references we refer the reader principally to [1],[2]. Generally, as in [1],[2], we will unless otherwise stated assume a zero Dirichlet boundary condition: $v = 0$ on $\partial\Omega$.

There are many discretizations that one can use: piecewise linear, piecewise quadratic, and so on. Here we will focus attention to piecewise quadratic functions defined on each element τ in the triangulation of Ω , continuous across the boundaries $\partial\tau$ between elements, and satisfying a weak form of (1.2):

$$\int_{\tau} \nabla\cdot v = 0 \tag{2.1}$$

on each τ . This is called the APX2 approximation in [1].

As an example, consider the solenoidal vector field

$$v = \left(\sin\pi(x_1+x_2),\ -\sin\pi(x_1+x_2)\right) \tag{2.2}$$

on the right triangle τ defined by the vertices

$$A_0 = (0,0)\ ;\ A_1 = (1,0)\ ;\ A_2 = (0,1)\ . \tag{2.3}$$

The quadratic vector field $v_h = (v_1,v_2)$ agreeing with v at the three corners and midedges of τ and also satisfying the weak solenoidal condition (2.1) may be seen to be:

$$v_h = \left(4(1-x_1-x_2)(x_1+\frac{3}{\pi}x_2),\ 4(1-x_1-x_2)(-\frac{3}{\pi}x_1-x_2)\right)\ . \tag{2.4}$$

The manner of construction uses barycentric coordinates and the decomposition described in Section 4.

3. Solenoidal subspaces. A fundamental problem from [1] resolved in [2] was the following. Given a triangulation of Ω and on it a finite element approximation scheme for the Navier-Stokes equations as outlined above, what is the

dimension of the subspace of approximating functions. Let us continue with just the APX2 scheme and Dirichlet zero boundary condition here, although the method of [2], which employs graph theory, may be used for other approximation schemes, as was done in [2].

Theorem [2]. (3.1)

dim(APX2) = 3 (the number of interior vertices of the triangulation)
+ (the number of interior midedges of the triangulation)
+ (the number of holes in the triangulation)

As an example, consider the triangulated domain Ω with 24 elements as shown in Fig. 1. By (3.1) the dimension of the conforming (i.e. continuous) piecewise quadratic APX2 solenoidal subspace is

$$3(3) + 27 + 1 = 37 \tag{3.2}$$

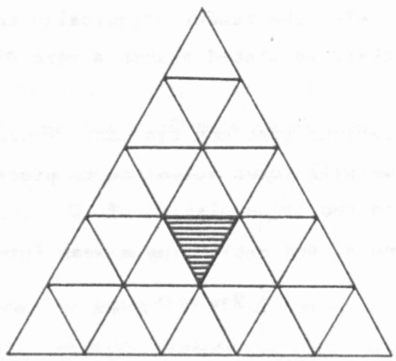

Fig. 1. A triangulated domain.

By contrast, if one lowers the order of approximation to a piecewise linear nonconforming solenoidal subspace (APX5 of [1]) one only reduces the dimension [2] to 31. There is a tendency in aerospace computer-aided design to use piecewise linear approximants, if they can get away with it. Accepting the bookkeeping headaches, the dimension results of [2] generally show that there is not much more storage required to go to higher order approximation.

Let us draw here a hypothetical airplane design triangulation as shown in Fig. 2. It is understood that the grid continues symmetrically to the left side of the figure. Actual design uses refined and complicated grid generation and graphics methods, subjects in themselves. We don't want to get into those aspects here. But just to generate a feeling for dimension, we find that for the situation depicted in Fig. 2 one has dimension

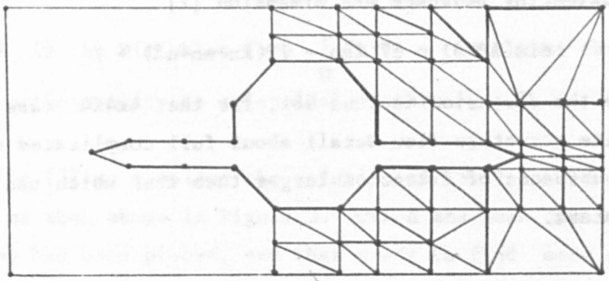

Fig. 2. Aircraft design domain.

$$\dim(APX2) = 3(46) + 188 + 1 = 327 \tag{3.3}$$

whereas

$$\dim(APX5) = 46 + 188 + 1 = 235 \tag{3.4}$$

That is, in two dimensions the dimension of the continuous piecewise quadratic solenoidal approximating subspace differs [2] from the discontinuous piecewise linear solenoidal approximating subspace only by 2 (number of interior vertices), the dominant part of the dimension being the interior midedge count.

One should not be misled by these small dimensions. For the two-dimensional cross-sectional design of a single part of an aircraft it is not unusual to see $0(10^4)$ elements used. The dimension of most of the finite element solenoidal approximating subspaces is seen to be of the same order. One should think therefore in terms of approximation by subspaces of large dimension.

Going from two to three dimensions increases the memory requirements dramatically. Cut a cube into 27 smaller cubes and then triangulate each of the smaller cubes into 5 tetrahedra to arrive at a 135-element triangulation. By [2] the dimension of the piecewise linear scheme APX5 is

$$\dim(APX5) = 25\,\ell mn - 6(\ell n + mn + n\ell) + 1 \tag{3.5}$$

where ℓ, m, and n denote the number of mesh intervals on each side of the cube. In the example cited, the dimension is thus

$$25(3)^3 - 6(3)(9) + 1 = 514\ . \tag{3.6}$$

Going to a 4x4x4 cube then triangulated produces a solenoidal APX5 subspace of dimension 1313.

We may compare APX3, the piecewise cubic approximation in three dimensions that is constructed [1] analogously to APX2. For the $\ell \times m \times n$ cube then triangulated the solenoidal approximating subspace has dimension [2].

$$\dim(\text{APX3}) = 37\,\ell mn - 12(\ell n + mn + n\ell) + 7 \tag{3.7}$$

For the 3x3x3 case the dimension is thus 681, for the 4x4x4 case it is 1799.

Capture of finite structure flow detail about full complicated configurations currently requires subspaces of dimension larger than that which can be accommodated on present day computers.

4. Subspace substructure. A key step in the subspace dimension theory of [2] is the decomposition of the solenoidal subspaces according to the Helmholtz decomposition

$$V = V_1 + V_2 + V_3 \tag{4.1}$$

where

$$\begin{aligned} \nabla \cdot v_1 &= 0 \quad \text{and} \quad \nabla \times v_1 = 0 \\ \nabla \cdot v_2 &= 0 \quad \text{and} \quad \nabla \times v_2 \neq 0 \\ \nabla \cdot v_3 &\neq 0 \quad \text{and} \quad \nabla \times v_2 = 0 \end{aligned} \tag{4.2}$$

One might object that the vector fields are solenoidal already, but the decomposition is performed on faces and sides, i.e., on manifolds of lower dimension. See [2].

The dimension is then found as the sum of the dimensions of the subspaces V_1, V_2, and V_3. Thus each solenoidal approximating subspace of finite element shape functions of any given scheme can be broken down into three subspaces;

$$\begin{aligned} &\text{subpotential component} \\ &\text{subsolenoidal component} \\ &\text{subrotational component} \end{aligned} \tag{4.3}$$

For example, the APX5 schemes have no subpotential component, and it is by that amount that they differ from the APX2 and APX3 higher order approximation schemes.

5. Linear algebra. Rather than consider the full time dependent nonlinear Navier-Stokes momentum equation (1.1) let us consider here the stationary linear Stokes problem

$$-\Delta u = -\nabla p + f \quad \text{in} \quad \Omega \tag{5.4}$$

with zero Dirichlet boundary conditions. This is placed in the weak form:

$$a(u,v) = (f,v) \tag{5.5}$$

for all v such that

$$\begin{cases} \nabla\cdot v = 0 & \text{in } \Omega \\ v = 0 & \text{on } \partial\Omega \end{cases} \tag{5.6}$$

Here $a(u,v)$ is the Dirichlet form $\int_\Omega \nabla u\cdot\nabla v$. Note that the pressure gradient vanishes by orthogonality to solenoidal vectors.

Following [3] we consider the solution of (5.4) in weak form (5.5) on a simple domain such as that shown in Figure 3. Given any such domain on which a triangulation has been placed, one then needs to find once and for all the matrix

$$[a(c_i,c_j)] \tag{5.7}$$

in which the c_i are a cycle basis for the solenoidal approximating subspace chosen. From this (5.5) may then be solved for any data f.

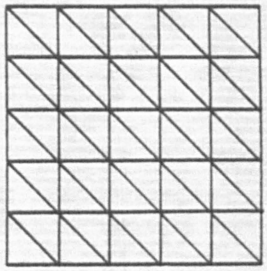

Fig. 3. Stokes problem domain.

Methods for finding cycle bases are discussed in [2,4,5]. For the domain of Figure 3, the 50 elements with piecewise quadratic approximating scheme APX2 placed thereupon produces a shape function subspace of dimension 113. The basis matrix (5.7) is shown in Figure 4, with $a_{ij} = 1$ meaning a nonzero entry and $a_{ij} = 0$ meaning a zero entry. The matrix is symmetric and contains a couple of errors due to roundoff during its computation on a Vax 11-780. Note the good sparseness of the matrix.

6. Divergence-form equations. Uniformly elliptic operators

$$Lu = \nabla\cdot(a\nabla u) = 0 \tag{6.1}$$

and finite difference methods may be treated by the same methods. Consider as an example the discretized problem

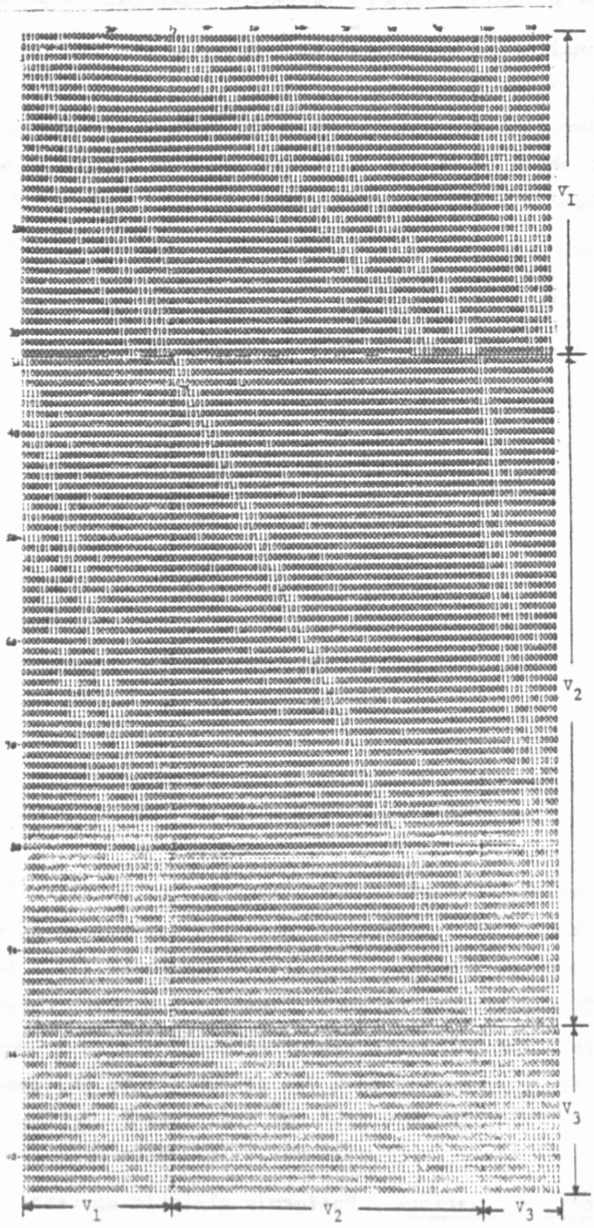

Fig. 4. Basis matrix, with subsubspaces shown.

$$\begin{cases} \Delta_h u = 0 & \text{in } \Omega \\ u = g & \text{on } \partial\Omega \end{cases} \tag{6.2}$$

where Δ_h denotes the standard five point centered difference Laplacian on the domain of Fig. 5 with the boundary values of g shown there.

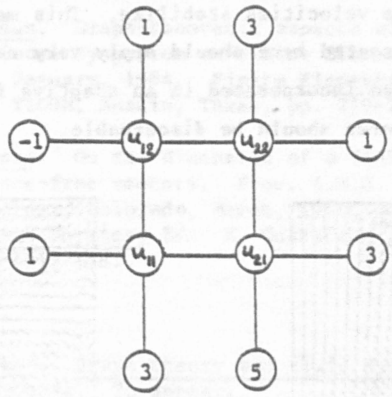

Fig. 5. Dirichlet problem.

By first forming discrete gradients ∇u and then applying the solenoidal subspace theory to the quantities $a\nabla u$ one finds approximate solutions of (6.1). For the example (6.2), following [6] one obtains, after a boundary identification, a finite difference approximating subspace of dimension 8. From this, in a manner somewhat similar to that described in Section 5 above, one may solve the example (6.2) to obtain the solution

$$(u_{11}, u_{12}, u_{21}, u_{22}) = (2,1,3,2) \tag{6.3}$$

Further details may be found in [5,6].

7. Graphs and networks. A main idea of [2] may be described, roughly and in hindsight, as the application of graph and network theory to fluid dynamics. In [7] we reverse the order and investigate the application of fluid dynamics to graph and network theory. In particular in [7] we so initiate a corresponding classification and structure theory for graphs.

8. Fluid dynamics. The potential viability of these methods to general fluid dynamics problems may be illustrated by looking at the fluid flow patterns in Figs. 6,7 . These [8,9] are time dependent full Navier-Stokes flows followed by a finite difference (marker and cell) method. The physical domain is a cavity with a lid moving uniformly to the left with velocity $v = (-1,0)$ and with zero Dirichlet boundary conditions maintained on the other three sides. The results agree to the discernable accuracy with other numerical studies and physical observation.

In Figs. 6, 7, the velocities have been normalized to length one regardless of true amplitude. The amplitudes in the lower portions of the cavities are much smaller than the $O(1)$ amplitudes near the top. For example the intensity of the first corner eddy is $O(10^{-3})$ compared to the principal vortex.

A main point to make here is that the rotational patterns shown develop very early in the flow, well before the velocities stabilize. This means that cycle bases and the general methodology presented here should apply very naturally to such problems. In particular when incorporated in an adaptive finite element scheme, a number of fine fluid structures should be discernable.

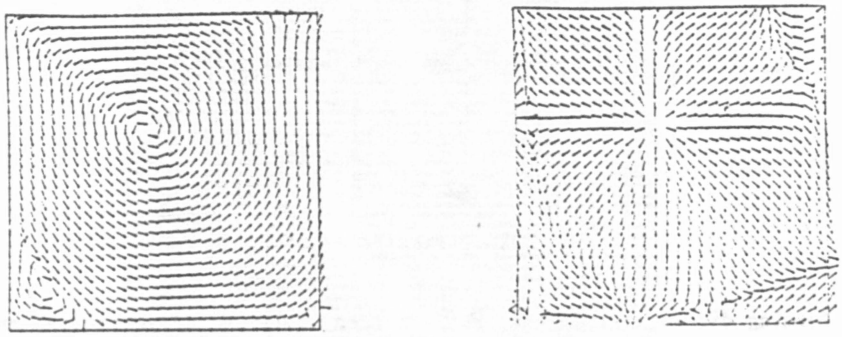

(a) Normalized Velocity Field (b) Normalized Pressure Gradient

Fig. 6. Basic cavity flow driven to near steady state, [8].
Full incompressible Naviet-Stokes equations at Re = 400.
Top lid moves uniformly to left with $v = (-1,0)$.

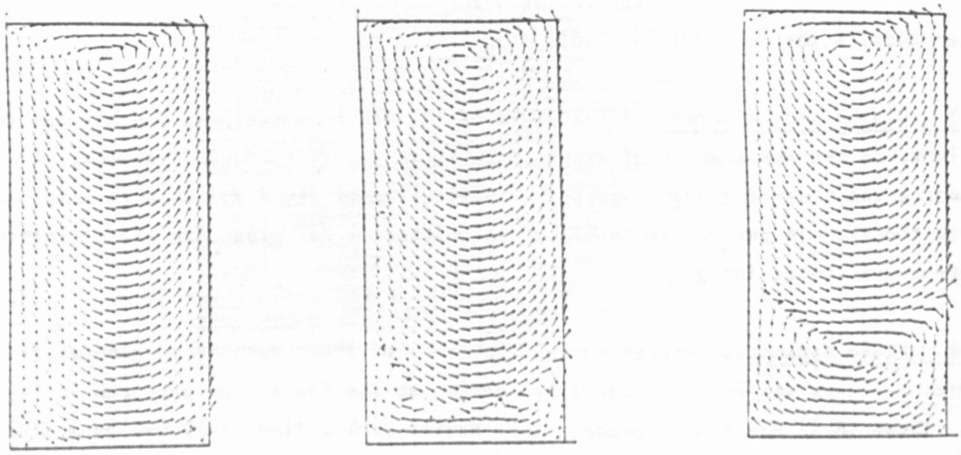

(a) 500 Δt (b) 1000 Δt (c) 2000 Δt

Fig. 7. Corner eddy dynamics in linear Stokes flow [9] .
Aspect ratio depth/width = 2 , Re = 400, Δt = 0.02.
(a) Corner eddies develop. (b) Corner eddies coalesce (c) Two principal vortices.

References

1. R. Temam. Navier-Stokes equations. Elsevier-North Holland, New York, 1979.

2. K. Gustafson and R. Hartman. Divergence-free bases for finite element schemes in hydrodynamics. SIAM J. Numerical Analysis, Vol. 20, pp. 697-721, 1983.

3. K. Gustafson and R. Hartman. Graph-theoretic aspects of flow calculation methods. Fifth International Symposium on Finite Element Methods in Flow Problems, Austin, Texas, January, 1984. Finite Elements and Flow Problems Eds.: G. Carey, J. Oden, TICOM, Austin, Texas, pp. 219-223, 1984.

4. R. Hartman and K. Gustafson. On the dimension of a finite difference approximation to divergence-free vectors. Proc. A.M.S. Special Session in Mathematical Physics, Boulder, Colorado, March, 1980, Quantum Mechanics in Mathematics, Chemistry, and Physics, Eds: K. Gustafson and W. Reinhardt, Plenum Press, New York, pp. 125-131, 1981.

5. K. Gustafson. To appear.

6. K. Gustafson and R. Hartman. Graph theory and fluid dynamics. SIAM J. Albebraic and Discrete Methods. To appear.

7. K. Gustafson and F. Harary. The curl of graphs and networks. Mathematical Modelling. To appear, 1984.

8. K. Gustafson and K. Halasi. Vorticity, incompressibility, and boundary conditions in the numerical solution of the Navier-Stokes equations. Proc. Int. Conf. on Differential Equations, Birmingham, Alabama, March, 1983. Ed.: I. Knowles and R. Lewis, North Holland, Amsterdam, 1984.

9. K. Gustafson and K. Halasi. Aspects of the driven cavity problem. To appear.

Department of Mathematics
University of Colorado
Boulder, Colorado 80309 USA